

Observation of topological charge pair nucleation in parametric wave mixing

Dmitri V. Petrov and Lluís Torner

Laboratory of Photonics, Department of Signal Theory and Communications, Universitat Politècnica de Catalunya, Gran Capitan UPC-D3, Barcelona ES 08034, Spain

(Received 3 December 1997; revised manuscript received 19 May 1998)

We report the observation of the nucleation of pairs of screw dislocations of opposite topological charges in second-harmonic generation processes in quadratic nonlinear media. The observation provides evidence about the conservation and evolution of the topological charge of light waves parametrically interacting in the nonlinear medium in the dynamical regime explored. [S1063-651X(98)12111-6]

PACS number(s): 42.65.Tg, 03.40.Kf, 42.65.Ky

Topological wave front dislocations are ubiquitous entities that play an important role in many branches of science [1]. They appear in different areas of both classical and quantum physics, including condensed matter, fluid dynamics, superconductivity, and optics. Besides their fundamental far-reaching importance, wave front dislocations have potential practical applications in fields as diverse as oceanography, information processing, or biology [1–6]. Here we address dislocations of optical waves which appear in different settings and materials.

Screw dislocations, or vortices, are a common wave front dislocation type. They appear as spiral phase ramps around a singularity where the phase of the wave is undefined thus its amplitude must vanish. The order of the singularity multiplied by its sign is referred to as the *topological charge* of the dislocation. Because of the topological stability of the corresponding dislocations, in the case of ideal “dark” fields that extend to infinity in the transverse directions, the net charge of the existing dislocations is conserved during the wave propagation in a linear continuous medium. Such is not necessarily the case with “bright,” finite-size inputs whose amplitude decays far from the beam center, because in such a case charges might move away and disappear, or on the contrary come from the beam tails, as recently shown by Soskin and co-workers [7]. However, one expects the dynamic creation or annihilation of dislocations in regions with a finite field amplitude to occur in pairs of oppositely charged vortices, hence with a vanishing net charge. To the best of our knowledge, all previous investigations support this expectation. This includes the fascinating case of speckle and random fields that were found to contain a high density of dislocation pairs of opposite charges [8–10], and also single-frequency wave propagation in cubic and photorefractive nonlinear media in single-pass and cavity configurations [5–6,11–17].

Parametric, nonlinear mixing of multiple waves containing wave front dislocations constitutes a totally new scenario. Because of the parametric interaction, the waves exchange not only energy with each other but also nonlinear phase shifts, hence wave fronts. Therefore a general question arises about the evolution of the topological charges existing in the waves. Taking into account the behavior obtained in linear media, such evolution and in particular the number of dislocations present, is expected to depend on the nonlinear competition between the various features of the interacting waves, in terms of shapes, widths, peak amplitudes, relative

phases, or nonlinear coupling type and strength. To start such a wide program, we identified and experimentally explored a particular regime where *pairs of screw dislocations are spontaneously nucleated* in such a way that the topological charge is conserved for each of the interacting waves. The aim of this paper is to report our observations. Second-harmonic generation of light in quadratic nonlinear media under appropriate conditions provides the required physical setting. In this process, one or two fundamental waves at frequency ω and one second-harmonic wave at frequency 2ω generate each other and parametrically mix in the nonlinear medium.

In upconversion of fundamental signals with moderate input powers and wide beams, light undergoes frequency doubling together with the generation of a phase dislocation nested in the second-harmonic beam, a phenomenon that has been observed experimentally [18–20]. The topological charge of the dislocation generated is dictated by the charge of the input light. However, this case does not give any information about the topological charge conservation in the sense described above, because *initially the second-harmonic wave does not exist*. Hence, its initial topological charge is undefined. A totally different situation is encountered when a coherent second-harmonic wave, with a well-defined topological structure, is also input at the crystal together with the fundamental beams. Our plan was to study the topological charge evolution in this case. Next, we describe the experimental setup that we have designed with this goal in mind and the outcome of the observations.

The experiments were designed with the following guidelines. First, only light at the fundamental frequency will be launched in the nonlinear crystal, and the topological charge of the generated second-harmonic wave will be monitored using interferometric techniques. Then, a weak second-harmonic seed will be col launched with the fundamental and the topological structure of the output will be analyzed and compared with the previous one. The material and input light intensities will be chosen to yield low depletion of the pump wave and weak interaction between the waves, therefore only changes in the wave front of the double-frequency wave are expected. Otherwise, in highly nonlinear regimes the parametric mixing produces large nonlinear amplitude and wave front modulations that might make difficult the detection of the dislocations in the interferometric measurement.

Experiments were performed in the presence of diffraction and Poynting-vector walk-off with a 2 cm long

KTiOPO₄ (KTP) crystal cut for type II phase matching. In this geometry one of the fundamental waves is ordinary polarized while the second one is an extraordinary wave. A *Q*-switched Nd:YAG laser (YAG denotes yttrium aluminum garnet) was used to provide coherent 8 ns pulses with a spatial Gaussian shape at the fundamental (1.064 μm) and second-harmonic frequencies.

First we report the summary of the numerical simulations that we have performed to investigate the dynamics of the process. The evolution equations for the slowly varying field envelopes in the type II configuration can be written as

$$\begin{aligned} i \frac{\partial a_1}{\partial \xi} - \frac{\alpha_1}{2} \nabla_{\perp}^2 a_1 + a_3 a_2^* \exp(-i\beta\xi) &= 0, \\ i \frac{\partial a_2}{\partial \xi} - \frac{\alpha_2}{2} \nabla_{\perp}^2 a_2 - i\vec{\delta}_2 \cdot \vec{\nabla}_{\perp} a_2 + a_3 a_1^* \exp(-i\beta\xi) &= 0, \\ i \frac{\partial a_3}{\partial \xi} - \frac{\alpha_3}{2} \nabla_{\perp}^2 a_3 - i\vec{\delta}_3 \cdot \vec{\nabla}_{\perp} a_3 + a_1 a_2 \exp(i\beta\xi) &= 0, \end{aligned} \quad (1)$$

where a_1 , a_2 , and a_3 are the normalized envelopes of the ordinary-polarized fundamental wave, the extraordinary-polarized fundamental wave, and the second-harmonic wave, respectively. The parameters α_ν , with $\nu=1,2,3$, are the ratios of the linear wave numbers k_ν of the waves. In practice $\alpha_1 = -1$, $\alpha_2 \approx -1$, and $\alpha_3 \approx -0.5$. The transverse coordinates are normalized to a beam width η , and the propagation coordinate is normalized to the diffraction length $l_d = k_1 \eta^2 / 2$. The parameter β is given by $\beta = k_1 \eta^2 \Delta k$, where $\Delta k = k_1 + k_2 - k_3$ is the wave vector mismatch. The parameters $\vec{\delta}_{2,3}$ account for the presence of Poynting-vector walk-off. Notice that at first approximation, one could simplify Eqs. (1) by assuming negligible pump depletion, no diffraction, and no walk-off. However, even though such a reduced model might provide valuable information, the evolution of phase dislocations in multiple light beams depends critically on the relative sizes, positions, and amplitudes of the beams, even in linear media [7]. Therefore, with the aim to simulate the actual conditions present in experimental setup, we studied the full system (1).

We studied numerically the evolution of input beams with the form $a_\nu(\xi=0) = A_\nu \rho^{|m_\nu|} \exp(im_\nu \varphi) \exp(i\phi_\nu) \exp(-\rho^2/w_\nu^2)$, where ρ is the radial cylindrical coordinate, φ is the azimuthal angle, A_ν , w_ν , and ϕ_ν are the amplitudes, widths, and global phases of the light beams, respectively, and m_ν are the topological charges of the existing screw dislocations. Throughout the paper different combinations of charges are labeled by the value of the array $[m_1, m_2, m_3]$, and a big dot in the position of a m_ν indicates that the corresponding beam is not initially supplied. To analyze the presence of screw wave front dislocations we monitored the interference pattern arising by superposing the evolving beams with a reference plane wave tilted slightly relative to the propagation axis. The resulting scaled wave amplitude exhibits a characteristic fork at the position of the wave front dislocation and its topological charge is visually evaluated [21]. Further, we verified that the amplitude of the field vanishes at the location of the dislocation.

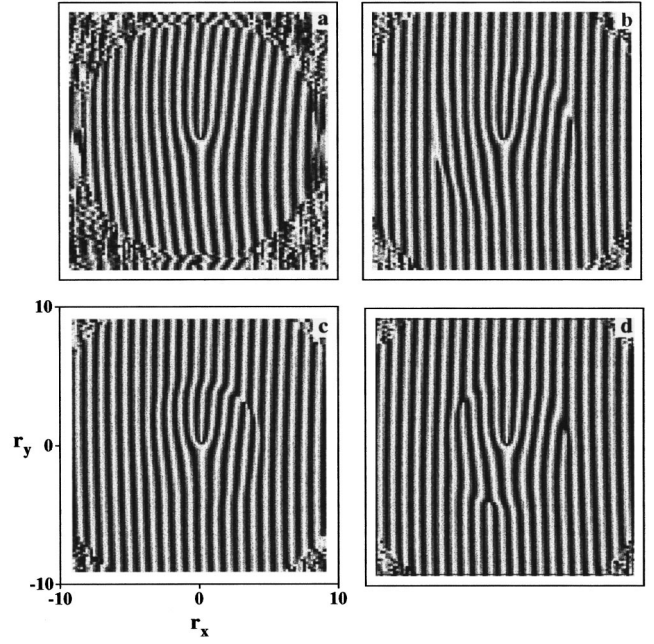


FIG. 1. Numerically obtained interferograms of the output second-harmonic light wave and a tilted plane wave showing the presence of screw dislocations, as described in the text. The parameters r_x and r_y are the transverse normalized coordinates. Conditions: $A_{1,2}=1$, $A_3=0.01$, $w_\nu=2$, $\beta=3$, and $\xi=0.2$. Topological charge combinations: (a) $[1,1,\bullet]$; (b) $[1,1,0]$; (c) $[1,1,1]$; (d) $[1,1,-1]$.

Simulations were performed by solving Eqs. (1) for a wide variety of material and input light conditions. For the sake of simplicity, we considered only the case of equal widths w_ν of the three input beams. Figures 1 and 2 show a summary of the outcome of the numerics. Figure 1 shows the

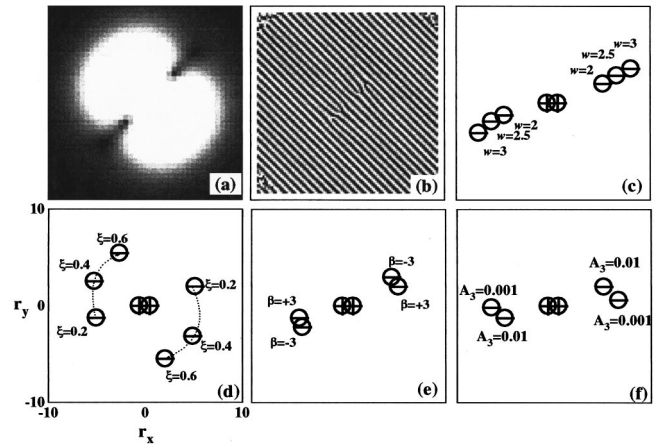


FIG. 2. Dynamics of the dislocations observed in the simulations. All plots correspond to the combination $[1,1,0]$, and unless otherwise stated $A_{1,2}=1$, $A_3=0.01$, $w_\nu=2$, $\beta=3$, and $\xi=0.2$. The parameters r_x and r_y are the transverse normalized coordinates. (a) Amplitude of the second-harmonic beam at $\xi \approx 0$ showing the nulls where dislocation ‘‘twins’’ appear; (b) interferogram capturing the instant when the twins self-split; (c)–(f) Sketches of the evolution of the dislocations with varying beam width, propagation distance, wave vector mismatch, and amplitude of the always small second-harmonic seed.

interferograms for the second-harmonic wave obtained for representative input conditions at a fixed propagation distance, but for different combinations of input topological charges. Figure 1(a) corresponds to the case $[1,1,\bullet]$. A dislocation with topological charge $m_3 = m_1 + m_2$ (in this case $m_3 = 2$) is generated in the second-harmonic beam. In contrast, Figs. 1(b)–1(d) show the interferograms obtained when a weak second-harmonic seed with a width equal to that of the initial fundamentals is input with different topological charges. Figure 1(b) corresponds to the case $[1,1,0]$ where the input second harmonic is a vorticityless Gaussian beam. One observes in the plot that in addition to the dislocation with charge $+2$ present in Fig. 1(a) there are two single-charge dislocations with charge -1 . Thus the net charge is zero as in the original input beam. Analogous features are seen in Figs. 1(c) and 1(d) for the cases $m_3 = \pm 1$. Changing the values of the various parameters involved modifies the details of the wave evolution but we always observed the same number of dislocations. Some representative cases are shown in Fig. 2, which concentrates on the case $[1,1,0]$. In the negligible pump-depletion conditions examined in this paper, no changes in the number of dislocations existing in the wave front of the fundamental beams were ever found. Analogous results were obtained for all the combinations of topological charges considered.

The dynamics of the charges can be summarized as follows. The second-harmonic light that is generated in the presence of the initial seed produces the amplitude pattern shown in Fig. 2(a). In two nulls located symmetrically around the propagation axis two pairs of dislocations appear, each pair with zero topological charge. Such “twins” then split into the positive and the negative charges that they contain. The positive charges move inwards, towards the propagation axis, whereas the negative charges move outwards [Fig. 2(b)] till they reach a circle located at a few beam widths. Increasing the input beam width increases the distance of the negative charges from the origin [Fig. 2(c)]. For a given width, when the propagation distance further increases and the beams diffract the charges rotate clockwise around the origin [Fig. 2(d)]. For other combinations of input charges where the outer charge is positive, e.g., $[1, -1, 1]$, it rotates anticlockwise. Going back to the case $[1, 1, 0]$, by and large, changing the value of the wave vector mismatch [Fig. 2(e)], the global phases ϕ_ν of the beams, or the presence of Poynting-vector walk-off (e.g., setting $\delta_{2,3} \approx 1$), modifies the azimuthal symmetry of Fig. 2(a) and this changes the location of the charges accordingly. Similarly, increasing the energy of the second-harmonic seed, or decreasing the energy of the pump fundamental wave, reduces the distance between the positive and negative charges [Fig. 2(f)]. Finally, addition of random noise to the inputs modifies the details of the output pattern but not its main features.

Taking into account the behavior obtained for the mixing of beams with different topological charges propagating in linear media [7], one expects that different pump and seed input intensities, beam shapes and widths, or larger propagation distances might give a different outcome than the one described above. A detailed investigation of all such cases needs to be performed and shall be published elsewhere. However, the important point is that the above simulations suggest that under the conditions identified here, in the pres-

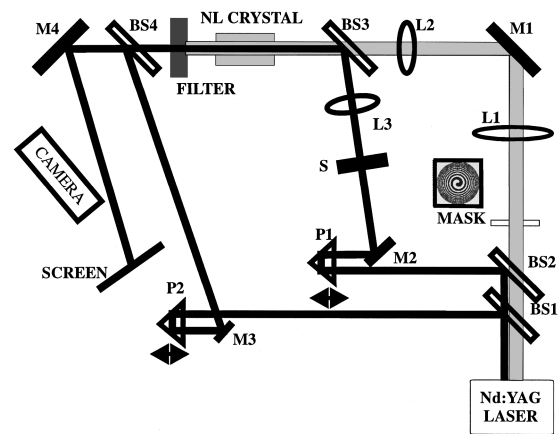


FIG. 3. Sketch of the experimental setup employed. NL stands for “nonlinear.”

ence of a suitable initial seed the second-harmonic light beam is generated in such a way that the topological charge of the input wave is conserved.

To investigate experimentally this prediction we employed the setup shown in Fig. 3 and operated it for the combination $[1,1,0]$. Single-charge topological screw dislocations were nested in the fundamental beams using computer-generated spiral zone plates [21]. A lens $L1$ allowed us to separate the beam with a nested vortex from the undiffracted light and higher-order Fresnel images [21]. Using the lens $L2$ light was focused to an approximately $60 \mu\text{m}$ waist at the entrance face of the KTP crystal. An optical attenuator was used to tune the input intensity. The fundamental input power was measured to be about 1 kW. The double-frequency beam from the laser was split into two beams by the beam splitter BS1. One of the two beams was used as a seed beam. It reflected from the dichroic mirror BS2, a mirror $M2$, and after a beam splitter BS3 it entered the KTP crystal parallel to the fundamental beam when the stop S was open. A lens $L3$ allowed us to match the sizes of both beams inside the KTP crystal. The second double-frequency signal was used as a reference wave to reveal the topological structure of the second-harmonic beam output of the KTP crystal. The intensity pattern of output light was analyzed by a charge coupled device (CCD) camera. The wave front of the beam was carefully scanned by changing the position of the reference wave using the beam splitter BS4. Prisms $P1$ and $P2$ were used to achieve temporal overlap of the fundamental and second-harmonic pulses in all channels.

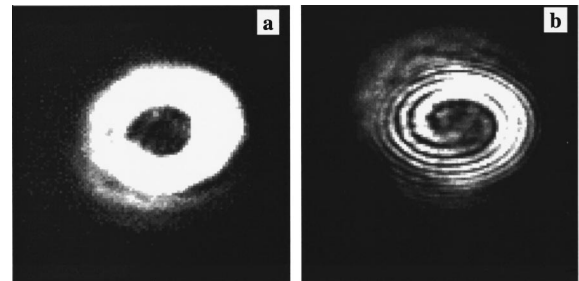


FIG. 4. Magnified image of light distribution at the SH frequency and interferogram in the case $[1,1,\bullet]$ observed on the screen (see Fig. 3) when the input beam is not focused. The size of the beam at the output of the crystal is about 3 mm.

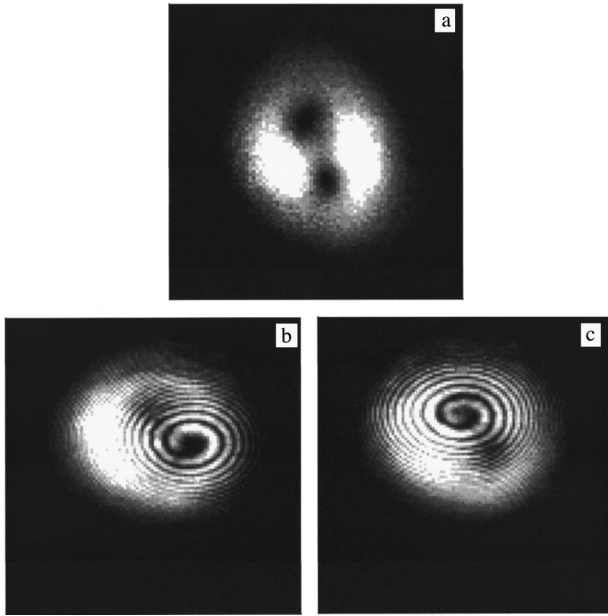


FIG. 5. Magnified image of light distribution at the SH frequency and interferograms in the case $[1,1,\bullet]$ observed on the screen when the input beam is focused to waist of some $60\ \mu\text{m}$. The size of the beam at the output of the crystal is about $200\ \mu\text{m}$. The interferograms were obtained by scanning the wave front of the output second-harmonic beam in different directions, and each picture corresponds to a different direction of the reference wave.

Figures 4(a) and 4(b) show the intensity and interferogram measured without second-harmonic seed and when the input fundamental beam was not focused. In this case the waist of the beam was about 3 mm. In agreement with previous measurements [18–20], and with Fig. 1(a), the double spiral of the interferogram reveals the presence of a dislocation of charge $+2$. Then, we focused the input fundamental beam, still without any second-harmonic seed. The output second-harmonic light, displayed in Fig. 5(a), and the corresponding interferograms displayed in Figs. 5(b) and 5(c), show that the double-charge dislocation has split into two $+1$ charges. This splitting is due to the instability of higher-order dislocations against symmetry breaking perturbations [16], and we believe that it is revealed here but it is not apparent in Fig. 4 because focusing the beams reduces the scale lengths at which the instability manifests itself. Inside the sensitivity limits of our experiments, we did not find any other dislocation in the wave front.

Now, with identical conditions we open the stop S and launch the second-harmonic seed into the crystal. Figures 6 show the intensity pattern [Fig. 6(a)] and interferograms [Figs. 6(b)–6(e)] measured. The presence of two dislocations with negative single charges in addition to the pair present in Fig. 5 is clearly visible. We carefully scanned the wave front and no additional dislocations were found. The positions of the two dislocations with positive charge did not change remarkably with the presence of the seed. The position of the additional charges was observed to depend strongly on the overlap between the input fundamental and seed beams and weaker on the intensity of the seed. The experiment was repeated for different light intensities, beam widths, crystal orientations, discrete elements of the experimental setup, and operation conditions of the laser, always inside the negligible

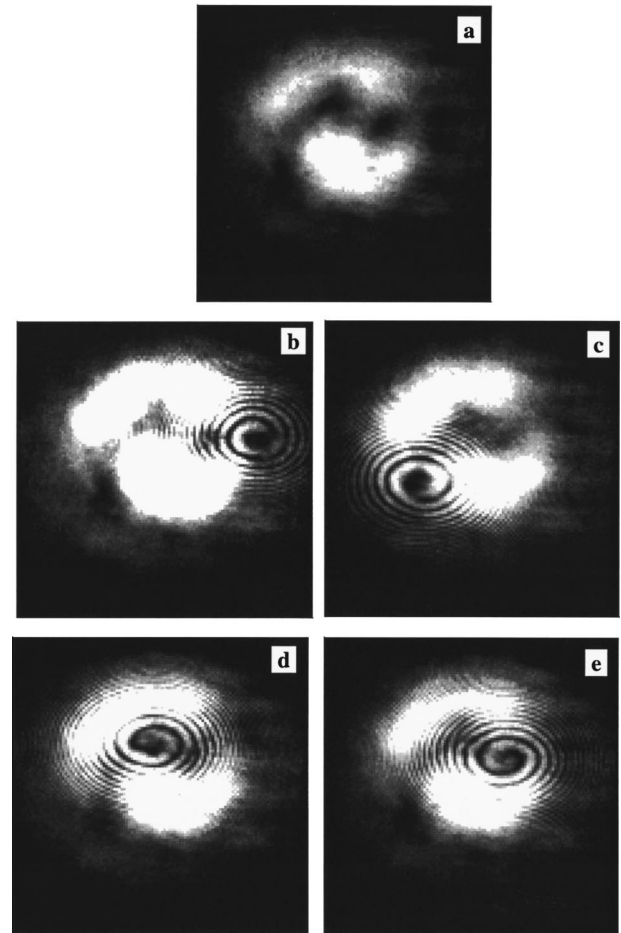


FIG. 6. Observed light distribution at the second-harmonic frequency and interferograms in the case $[1,1,0]$. The interferograms were obtained by scanning the wave front of the output second-harmonic beam in different directions, and each picture corresponds to a different direction of the reference wave.

pump-depletion regime and with almost equal widths of the pump and seed beams. Results analogous to those shown in Fig. 6 were always observed.

In conclusion, we reported experimental observations of the evolution of topological wave front charges of multiple light beams parametrically interacting in a quadratic nonlinear medium. We designed our experiments to involve weak signals and low depletion of the pump light, hence only the second-harmonic signal is affected by the wave interaction. Our observations suggest that in the experimental conditions we have explored here the topological charge is conserved for each of the waves. Different dynamical and input conditions, in terms of total and relative pump and seed energies, beam shapes and widths, or crystal length, might yield a different outcome [7]. Our result poses the fascinating challenge of the observation of the topological charge evolution under such different conditions, and in particular in high intensity regimes where the energy goes back and forth between the waves and induces strong nonlinear distortions of their wave fronts due to cascading [22].

This work was supported by the Spanish Government under Contract No. PB95 0768. We thank E. M. Wright, J. P. Torres, and A. A. Zozulya for suggestions, and F. Canal, M. C. Santos, and J. Rodriguez for assistance.

- [1] J. F. Nye and M. V. Berry, Proc. R. Soc. London, Ser. A **336**, 165 (1974); M. V. Berry, in *Physics of Defects*, edited by R. Balian, M. Kleman, and J.-P. Poirier (North-Holland, Amsterdam, 1981).
- [2] A. Ashkin, J. M. Dziedzic, and T. Yamane, Nature (London) **330**, 769 (1987).
- [3] M. Padgett and L. Allen, Phys. World **10**, 35 (1997).
- [4] H. He, M. E. J. Friese, N. R. Heckenberg, and H. Rubinstein-Dunlop, Phys. Rev. Lett. **75**, 826 (1995).
- [5] B. Luther-Davies, J. Christou, V. Tikhonenko, and Y. S. Kivshar, J. Opt. Soc. Am. B **14**, 3045 (1997).
- [6] D. Rozas, C. T. Law, and G. A. Swartzlander, J. Opt. Soc. Am. B **14**, 3054 (1997).
- [7] M. S. Soskin, V. N. Gorshkov, M. V. Vasnetsov, J. T. Malos, and N. R. Heckenberg, Phys. Rev. A **56**, 4064 (1997).
- [8] N. B. Baranova, B. Ya. Zel'dovich, A. V. Mamaev, N. F. Pilipetskii, and V. V. Shkunov, Zh. Eksp. Teor. Fiz. **83**, 1702 (1982) [Sov. Phys. JETP **56**, 983 (1982)].
- [9] F. T. Arecchi, G. Giacomelli, P. L. Ramazza, and S. Residori, Phys. Rev. Lett. **67**, 3749 (1991).
- [10] N. Shvartsman and I. Freund, Phys. Rev. Lett. **72**, 1008 (1994).
- [11] P. Coullet, L. Gil, and F. Rocca, Opt. Commun. **73**, 403 (1989).
- [12] G. A. Swartzlander and C. T. Law, Phys. Rev. Lett. **69**, 2503 (1992).
- [13] G. Indebetouw, J. Mod. Opt. **40**, 73 (1993); G. Indebetouw and D. R. Korwam, *ibid.* **41**, 941 (1994).
- [14] E. M. Wright, R. Y. Chiao, and J. C. Garrison, Chaos Solitons Fractals **4**, 1797 (1994).
- [15] N. R. Heckenberg, M. Vaupel, J. T. Malos, and C. O. Weiss, Phys. Rev. A **54**, 2369 (1996).
- [16] A. V. Mamaev, M. Saffman, and A. A. Zozulya, Phys. Rev. Lett. **77**, 4544 (1996); **78**, 2108 (1997).
- [17] Z. Chen, M. Segev, D. W. Wilson, R. E. Muller, and P. D. Maker, Phys. Rev. Lett. **78**, 2948 (1997).
- [18] I. V. Basistiy, V. Y. Bazhenov, M. S. Soskin, and M. V. Vasnetsov, Opt. Commun. **103**, 422 (1993).
- [19] K. Dholakia, N. B. Simpson, M. J. Padgett, and L. Allen, Phys. Rev. A **54**, R3742 (1996); J. Courtial, K. Dholakia, L. Allen, and M. J. Padgett, *ibid.* **56**, 4193 (1997).
- [20] A. Berzanskis, A. Matijosius, A. Piskarskas, V. Smilgevicius, and A. Stabinis, Opt. Commun. **140**, 273 (1997).
- [21] N. R. Heckenberg, R. McDuff, C. D. Smith, and A. G. White, Opt. Lett. **17**, 221 (1992).
- [22] G. I. Stegeman, D. J. Hagan, and L. Torner, Opt. Quantum Electron. **28**, 1691 (1996).